Choi-Williams time-frequency representation of acoustic signals

Abdelkader Elhanaoui, El Houcein Aassif, Gerard Maze

ACOUSTICS 2012

Choi-Williams time-frequency representation of acoustic signals

A. Elhanaoui[a], E.H. Aassif[a] and G. Maze[b]

[a]Université IBN ZOHR, BP 28/S, Faculté des Sciences, 80000 Agadir, Morocco
[b]LOMC, IUT, Université du Havre, Place Robert Schuman, Place Robert Schuman, 76610 Le Havre, France
agrgsp@yahoo.fr

This work concerns the study of acoustic signals that are backscattered by thin aluminum tubes filled by air and immersed in water. This study is done with Choi-Williams (CW) and smoothed pseudo Choi-Williams (SPCW) time-frequency representations. Choi-Williams representation is chosen to reduce the amplitude of the interferences in the time-frequency plane. This can make the interpretation of time-frequency image easier. However, the resolution of Choi-Williams time-frequency image is acceptable if the involved parameter is well chosen. As a result, the determination of longitudinal and transversal velocities values of aluminum reveals a good agreement with the theoretical method of proper modes of vibration as mentioned in scientific literature.

1 Introduction

The analysis of acoustic signals backscattered by thin tubes filled by air and immersed in water, is an important tool in the characterization domain. The theoretical and experimental studies have shown the dual relationship between the acoustic resonances of these targets and their geometric and physical properties [1.5]. The work we are presenting aims to measure physical characteristics of a thin aluminum tube filled by air and immersed in water with radii ratio b/a, where b and a denote the internal and the external radius successively. The length L of tube is supposed infinite (L>>a).

To solve this problem, we use a time-frequency analysis which shows representations in time and frequency all together. In this context, there is a multitude of solutions that we would like they meet certain properties. For many years, a particular interest is given to Wigner-Ville representation [8.9]. Nevertheless, some problems of interpretation seem to have curbed its use. CW representation is motivated by a desire to reduce the terms of interference while maintaining a good number of properties. The TFR mentioned above is applied to an experimental acoustic signal backscattered by a thin aluminum tube of radii ratio equal to 0.95. The paper is organized as follows. Section 2 is a brief introduction to acoustic scattering. In Section 3, we introduce the Cohen's class and give definition of CW representation. In Section 4, the treatment, following calculation of CW representation, consist to visualize the evolution of frequency over time of circumferential waves that propagate around the tube, and calculate physical parameters of aluminum. Results are obtained and fully discussed. Finally a conclusion is given in Section 5.

2 Acoustic scattering from an infinitely long tube

2.1 Modal representation

The acoustic scattering of an infinite plane wave by an infinitely long cylindrical tube with inner over outer radii ratio equal to b/a, is investigated through the solution of the wave equation and the associated boundary conditions. Figure1. shows the cylindrical coordinate orientation (r,θ,z) and the normal direction of a plane wave incident of an infinitely long tube in a fluid medium. The axis of the tube is taken to be the $z-$axis. The fluid (1) outside the tube has a density ρ_1 and propagation velocity c_1. The outer fluid (2) inside the tube is described by a density ρ_2 and propagation velocity c_2. Longitudinal and transversal waves velocities of tube's material are designed by c_L and c_T successively. The parameters of fluids inside and outside the tube are given in Table 1.

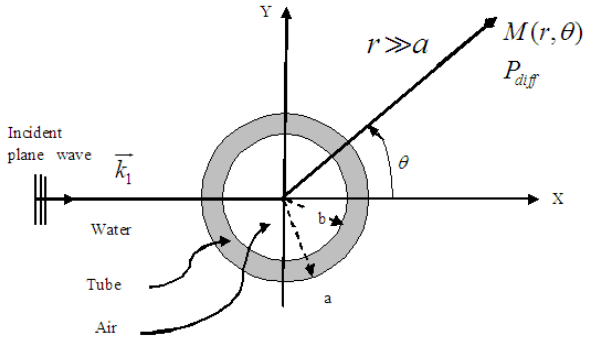

Figure 1: General geometry of backscattering of a plane wave by a thin tube filled by air and immersed in water.

Table 1: Fluid parameters.

Parameters	fluids	
	water	air
Density (kg. m^{-3})	1000	1.29
Phase velocity (10^3 m. s^{-1})	1.470	0.334

The mathematical approach is based on the Rayleigh series formation that consists of decomposition of scattered pressure field into an infinite summation of model components, depending on both physical properties and geometry of tube. The general form of scattered pressure field at normal incidence can be expressed as [11]:

$$P_{diff}(r,\theta) = P_0 \sum_{n=0}^{\infty} \left[R_n(\omega) \varepsilon_n H_n^{(1)}(k_1 r) \right] \cos(n\theta) \quad (1)$$

Where ω is the angular frequency. k_1 denotes the incident wave number with respect to wave velocity in external fluid. ε_n is the Neumann factor ($if\ n=0$, $\varepsilon_n=1$ $else\ \varepsilon_n=0$) . P_0 is the amplitude of the plane incident wave. Scattered coefficients $R_n(\omega)$ are computed from boundary conditions at both interfaces $r=a$ and $r=b$ .The function $H_n^{(1)}$ is called Hankel function of first kind.

The module of Hankel function in a faraway field can be expressed as:

$$\left|H_n^{(1)}(k_1 r)\right| \approx \sqrt{\frac{2}{\pi k_1 r}} \tag{2}$$

The module of scattered pressure in a faraway field is called form function F_∞ .The module of backscattered pressure in a faraway field is called backscattering spectrum and obtained by,

$$F_\infty(x_1) \approx \frac{2}{\sqrt{\pi x_1}} \left| \sum_{n=0}^{n_{\max}} (-1)^n \varepsilon_n R_n \right| \tag{3}$$

This form function is computed only in function of the reduced frequency x_1 expressed as:

$$x_1 = \frac{2\pi\nu}{c_1} a \,. \tag{4}$$

Figure 2. shows a typical form function for a thin aluminum tube of radii ratio 0.95. The succession of acoustic resonances is connected with propagation of circumferential waves:

- Scholte- Stoneley wave (A)
- Shell waves: A_1, A_2 … (Antisymmetric waves) and S_0, S_1, S_2 … (Symmetric waves).

Ccharacteristics of shell waves are related to the geometry and physical properties of the tube.

Figure3. shows the impulse response (temporal signal) for a thin aluminum tube filled by air and immersed in water, with radii ratio equal to 0.95.

2.2 Expressions of longitudinal and transversal velocities

Circumferential waves propagating around a thin elastic tube are identical to Lamb waves propagated in the plate [10]. Cutoff frequencies of symmetric (S) and anti

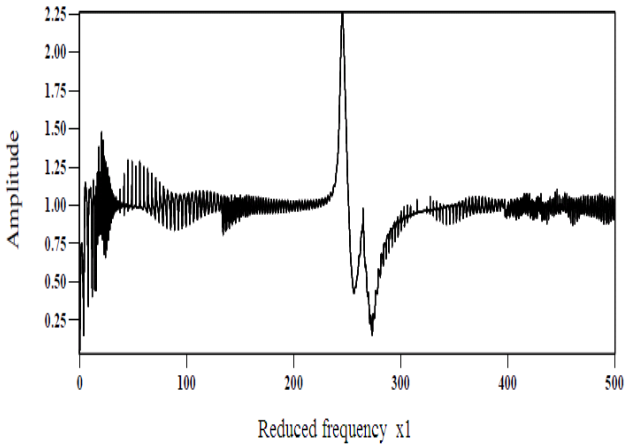

Figure 2: Form function for a thin aluminum tube of radii ratio 0.95 filled by air and immersed in water (a=0.03m).

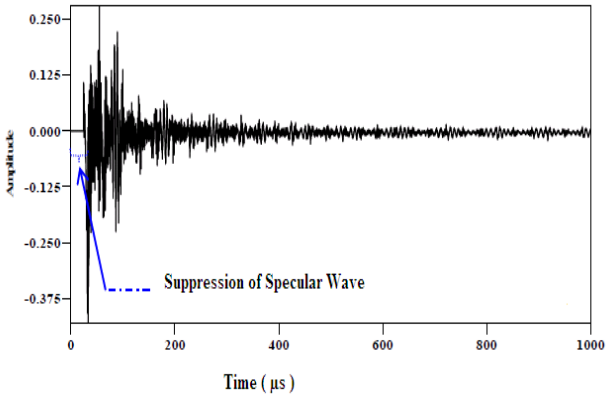

Figure 3: Impulse response of a thin aluminum tube of radii ratio equal to 0.95 filled by air and immersed in water (a=0.03m).

Symmetric (A) Lamb waves are given, as follows:

$$S_{2n}: \quad \nu_C = n.\frac{c_T}{e} \quad ; n=1,2,\ldots. \tag{5}$$

$$S_{2n+1}: \quad \nu_C = \left(n+\frac{1}{2}\right).\frac{c_L}{e} \quad ; n=0,1,2,\ldots. \tag{6}$$

$$A_{2n}: \quad \nu_C = n.\frac{c_L}{e} \quad ; n=1,2,\ldots. \tag{7}$$

$$A_{2n+1}: \quad \nu_C = \left(n+\frac{1}{2}\right).\frac{c_T}{e} \quad ; n=0,1,2,\ldots. \tag{8}$$

Where n and $e=a-b$ denote successively the circumferential wave mode and the thickness of tube. c_L and c_T represent respectively the longitudinal and the transversal velocities of the thin tube.

Cutoff reduced frequencies are obtained from Eq. (4),

Eq. (5), Eq. (6), Eq. (7) and Eq. (8).as follows,

$$S_{2n} \ : \quad x_{1C} = 2n \cdot \frac{c_T}{c_0} \ ; \ n = 1,2,.... \tag{9}$$

$$S_{2n+1} : \quad x_{1C} = (2n+1) \cdot \frac{c_L}{c_0} \ ; \ n = 0,1,2,.... \tag{10}$$

$$A_{2n} \ : \ x_{1C} = 2n \cdot \frac{c_L}{c_0} \ ; \ n = 1,2,.... \tag{11}$$

$$A_{2n+1} : \ x_{1C} = (2n+1) \cdot \frac{c_T}{c_0} \ ; \ n = 0,1,2,.... \tag{12}$$

Where:

$$c_0 = \frac{c_1\left(1 - \frac{b}{a}\right)}{\pi}. \tag{13}$$

The expressions of the longitudinal and the transversal velocities are deduced, as follows:

$$c_T = {x_{1C}}^{A_1} \cdot c_0 . \tag{14}$$

$$c_T = {x_{1C}}^{A_3} \cdot \frac{c_0}{3}. \tag{15}$$

$$c_L = {x_{1C}}^{S_1} \cdot c_0 . \tag{16}$$

3 Time- frequency representations

3.1 Cohen's class

In this section, we introduce the quadratic joint TFR known as Cohen's class. This class is defined, as follows [6.7]:

$$\begin{aligned} C_x(t,\nu) = & \iiint \Phi(t-s,\nu-\eta) \\ & \times x\left(s+\frac{\tau}{2}\right).x^*\left(s-\frac{\tau}{2}\right)e^{-j2\pi\eta\tau} \ ds d\tau d\eta \end{aligned}. \tag{17}$$

Where integrals are evaluated from $-\infty$ to $+\infty$ .In this equation, x^* is the complex conjugate of the signal x. Time and frequency are designed by t and ν respectively. $\Phi(\tau,\eta)$ is known the kernel. It determines the specific properties of different representations.

3.2 Choi-Williams representation

In order to reduce the cross-terms, CW representation uses the kernel that is expressed by an exponential form:

$$\Phi(\tau,\eta) = \exp\left(-\eta^2\tau^2/\sigma^2\right). \tag{18}$$

The parameter σ controls the amount of attenuation. If σ is large enough then the kernel approaches 1, CW representation approaches the Wigner-Ville representation (WV). For a small σ, it peaks at the origin and falls off rapidly away from the axis. This property contributes to suppressing cross-terms.

CW time-frequency representation is defined by [6.7]:

$$\begin{aligned} CW_x(t,\nu) = & \iint \frac{\sqrt{\sigma}}{2\sqrt{\pi}|\tau|} \cdot e^{\frac{-\sigma(s-t)^2}{16\tau^2}} \\ & \times x\left(s+\frac{\tau}{2}\right).x^*\left(s-\frac{\tau}{2}\right)e^{-j2\pi\nu\tau} \ ds d\tau \end{aligned}. \tag{19}$$

The discrete version of equation (19) for a sampled signal $x(n)$ is given, as follows:

$$CW_x[t,\nu] = 2\left\{\begin{array}{l} |x[t]|^2 + \sum_{\tau\neq 0}\sum_{s} \frac{\sqrt{\sigma}}{4\sqrt{\pi}|\tau|} e^{\frac{-\sigma(s-t)^2}{16\tau^2}} \\ \times z\left[s+\frac{\tau}{2}\right]\cdot z^*\left[s-\frac{\tau}{2}\right]e^{-j4\pi\nu\tau} \end{array}\right\}. \tag{20}$$

$z^*(t)$ denotes the complex conjugate of the analytic signal $z(t)$ associated to a signal $x(t)$.

Time-frequency smoothing (SPCW) can be achieved by

$$\begin{aligned} SPCW_x(t,\nu) = & \sqrt{\frac{2}{\pi}} \int h(\tau) \int g(t-s) \\ & \times \frac{\sigma}{|\tau|} e^{\frac{-2\sigma^2(s-t)^2}{\tau^2}} x\left(s+\frac{\tau}{2}\right)x^*\left(s-\frac{\tau}{2}\right)e^{-j2\pi\nu\tau} \ ds d\tau \end{aligned} \tag{21}$$

Where h and g are two windows. The discrete version of Eq. (21) for a sampled signal $x(n)$ is given as,

$$SPCW_x[t,\nu] = 2\left\{\begin{array}{l} h[0]g[0]|z[t]|^2 + \sum_{\tau\neq 0} h[\tau] \\ \left\{\sum_{\mu=-|\tau|}^{\mu=|\tau|} g[\mu]z[t+\mu+\tau].z^*[t+\mu-\tau]\right\}e^{-j4\pi\nu\tau} \end{array}\right\}. \tag{22}$$

4 Analysis of an acoustic signal backscattered by a thin aluminum tube

4.1 Time- frequency images

In this work, TFR including CW and SPCW are considered to reduce cross-terms and obtain better accuracy

of the time-frequency analysis. They are applied to an experimental acoustic signal backscattered by a thin aluminum tube of radii ratio 0.95. Figure 4. and Figures 5. display time-frequency images given by Eq. (20) and Eq. (22).

4.2 Results and Discussion

Fig. 4. and Figs. 5.represent time-frequency analysis results of the signal shown in figure 3., by applying CW and SPCW. From fig 4. it is seen that CW reduces considerably interferences in time-frequency plane. From fig 5(a), it is seen that frequency resolution is well when using SPCW with parameter σ large enough. However, time frequency image is not identified clearly because it does suffer from the problem of cross-terms which such as Wigner-Ville. From fig. 5 (b), it is found that cross-terms using SPCW for a small σ have been suppressed to some extent. Nevertheless, the frequency resolution by SPCW is not highest. From fig. 5(c), it is seen that cross-terms by SPCW for a smallest σ have been also restrained. The frequency resolution is found to be slightly better than that shown in fig. 5.(b). From fig. 5.(d)., the frequency resolution is found to be also accepted in comparison with that by Wigner-Ville representation.

Reduced cutoff frequencies of waves A1, S1 and A3, deduced by time-frequency images, are given in table 2.

They are considered to obtain the longitudinal and the transversal velocities values of aluminum. The results are presented in table 3.

From figure 6. , it is interesting to note that CW and SPCW time frequency representations permit to estimate longitudinal and transversal velocities values of aluminium with good precision(fewer than 3%).

Table 2: Reduced cutoff frequencies.

Reduced cutoff frequencies	Circumferential waves		
	A_1	S_1	A_3
x_{1c} Fig.4.	133.9	271.7	408
x_{1c} Fig.5 (a).	134	271.3	410
x_{1c} Fig.5 (b).	136.9	268.3	409
x_{1c} Fig.5 (c).	132.9	271.7	410
x_{1c} Fig.5 (d).	133.3	271.7	410

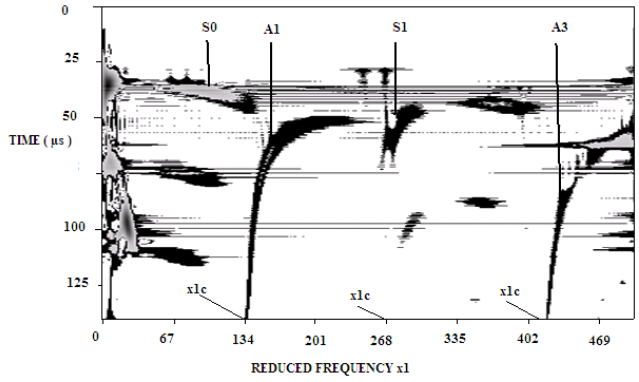

Figure 4: CW image of an acoustic signal obtained by the signal of Figure 3. (N=1024points; $\sigma = 1$).

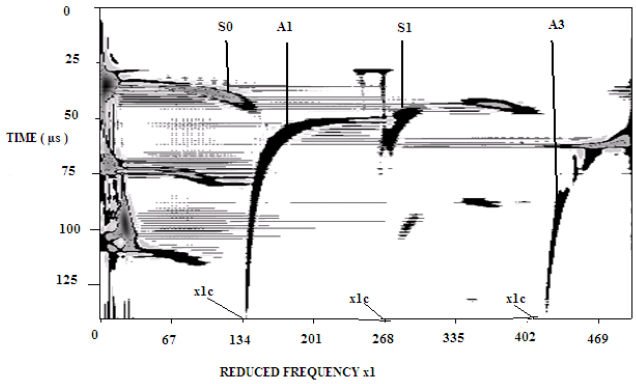

Figure 5(b): SPCW image of an acoustic signal obtained by the signal of Figure 3. (N=1024points; H=G=501; Blackman Harris windows; $\sigma = 20$).

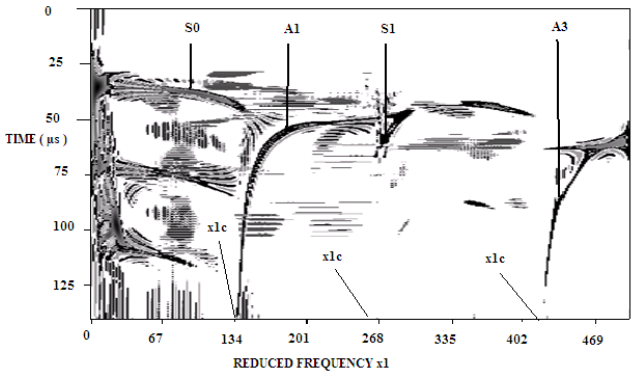

Figure 5(a): SPCW image of an acoustic signal obtained by the signal of Figure 3. (N=1024points; H=G=1023; Hamming windows $\sigma = 500$).

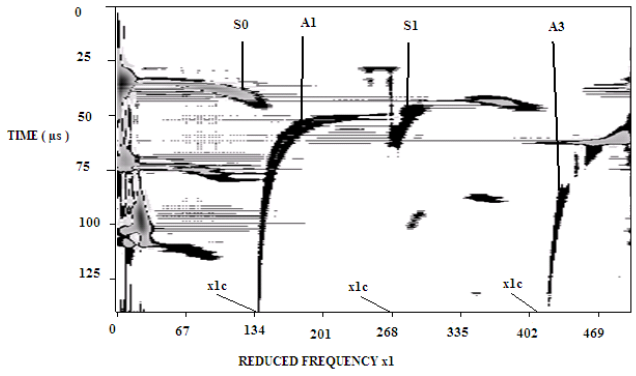

Figure 5(c): SPCW image of an acoustic signal obtained by the signal of Figure 3. (N=1024points; H=G=501; Blackman Harris windows; $\sigma = 10$).

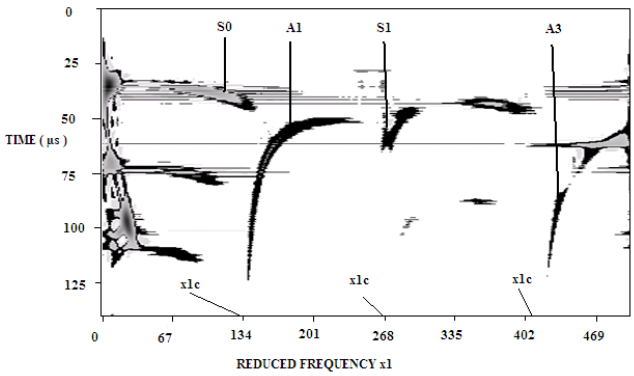

Figure 5(d): SPCW image of an acoustic signal obtained by the signal of Figure 3. (N=1024points; H=71;G=215; Hamming windows $\sigma = 3.6$).

Table 3: Longitudinal and transversal velocities values of aluminum.

Velocities values $(10^3 m.s^{-1})$	Circumferential waves		
	A_1	S_1	A_3
c_{t-f} Fig.4.	3.181	6.270	3.197
c_{t-f} Fig.5 (b).	3.202	6.277	3.189
c_{t-f} Fig.5 (c).	3.133	6.357	3.166
c_{t-f} Fig.5 (d).	3.119	6.347	3.197
$c_{p.m}$	3.100	6.380	3.100

5 Conclusion

In this paper, we demonstrate the particular interest of CW and SPCW time-frequency representations. These representations permit to reduce cross-terms and obtain better accuracy of the time-frequency analysis. CW and SPCW are applied to an experimental acoustic signal backscattered by a thin aluminum tube. As a result, we determinate the longitudinal and the transversal velocities values of aluminium. The comparison of these velocities and that calculated theoretically from the method of proper modes is in a good concordance. In continuation of this study maybe the investigation of defaults in tubes.

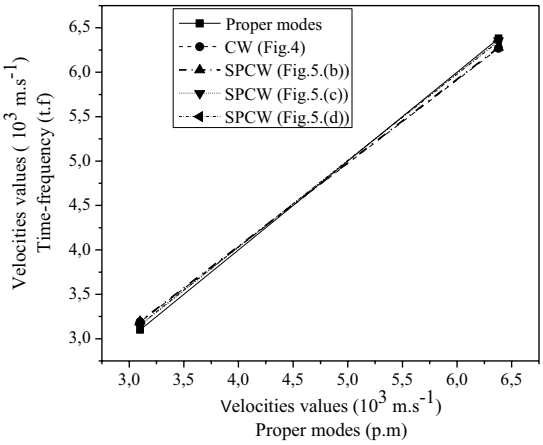

Figure 6: Correlation between Theoretical Velocities and Estimated Velocities values of aluminum.

References

[1] G. Maze, "Diffusion d'une onde acoustique plane par des cylindres et des tubes immergés dans l'eau, Isolement et Identification des Résonances", *Thèse de Doctorat d'état*, Rouen (1984)

[2] L. Haumesser, "Diffusion acoustique par des coques cylindriques limitées immergées, Ondes hélicoïdales : Analyse des réponses temporelles et Identification complète des Résonances ", *Thèse de Doctorat,* Le Havre (2001)

[3] O. Lenoir, "Diffusion acoustique impulsionnelle par des Multicouches planes immergés, Problème inverse, Détection des Résonances en présence d'Absorbants ", *Thèse de Doctorat,* Le Havre (1990)

[4] P. Delestre, J. L. Izbicki, G. Maze, J. Ripoche, "Excitation Acoustique Impulsionnelle d'une Plaque élastique Immergée : Application à l'Isolement des Résonances ", *Acoustica, N°61*, pp.83-85 (1986)

[5] G. Maze, B. Taconet, J. Ripoche, "Etude expérimentale des Résonances de Tubes Cylindriques remplis d'air immergés dans l'eau ", *Rev Du Cethedec., N°72*, pp.103-119 (1982)

[6] L. Cohen,"Time-frequency distribution",*a Revieu.Proc IEEE 77(7)*, 941-81 (1989)

[7] P. Flandrin et al, "Signaux non Stationnaires, Analyse Temps –Fréquence et Segmentation", *Traitement du signal Volume 9-Supplément au N°1,* (1992)

[8] R. Latif, E. Aassif, A. Moudden, B. Faiz , "High Resolution Time Frequency Analysis of an Acoustic Signal Backscattered by a Cylindrical Shell using a Modified Wigner- Ville Representation ", *Meas.Sci. Technol. 14*, pp.1063–1067 (2003)

[9] R. Latif, E. Aassif, G. Maze , D. Decultot, A. Moudden, B. Faiz, "Analysis of the Circumferential Acoustic Waves Backscattered by a Tube Using the Time Frequency Representation of Wigner-Ville", J. Measurement Science and Technology, Vol. 11,1 , pp.83–88 (2000)

[10] D. Royer, E. Dieulesaint, Ondes élastiques dans les solides, *Masson et Cie*, Tome 1, Paris (2000)

[11] N. Veksler, *Resonance acoustic spectroscopy*, Springer, Berlin (1993)